# Parametric analysis of a magnetized cylindrical plasma

Eduardo Ahedo[a)]
*Universidad Politécnica de Madrid, Madrid 28040, Spain*

(Received 10 September 2009; accepted 21 October 2009; published online 19 November 2009)

The relevant macroscopic model, the spatial structure, and the parametric regimes of a low-pressure plasma confined by a cylinder and an axial magnetic field is discussed for the small-Debye length limit, making use of asymptotic techniques. The plasma response is fully characterized by three-dimensionless parameters, related to the electron gyroradius, and the electron and ion collision mean-free-paths. There are the unmagnetized regime, the main magnetized regime, and, for a low electron-collisionality plasma, an intermediate-magnetization regime. In the magnetized regimes, electron azimuthal inertia is shown to be a dominant phenomenon in part of the quasineutral plasma region and to set up before ion radial inertia. In the main magnetized regime, the plasma structure consists of a bulk diffusive region, a thin layer governed by electron inertia, a thinner sublayer controlled by ion inertia, and the non-neutral Debye sheath. The solution of the main inertial layer yields that the electron azimuthal energy near the wall is larger than the electron thermal energy, making electron resistivity effects non-negligible. The electron Boltzmann relation is satisfied only in the very vicinity of the Debye sheath edge. Ion collisionality effects are irrelevant in the magnetized regime. Simple scaling laws for plasma production and particle and energy fluxes to the wall are derived. © *2009 American Institute of Physics*. [doi:10.1063/1.3262529]

## I. INTRODUCTION

The interaction of a small-Debye-length plasma with a material surface in the presence of a strong magnetic field $\boldsymbol{B}$ is a subject of high interest in different areas, such as tokamak plasmas, spacecraft-plasma interaction, plasma discharges, and plasma sources. The confinement and anisotropy introduced by the magnetic field makes one-dimensional (1D) asymptotic analyses of the problem still rich in phenomena because of the presence of several length scales, such as the Debye length $\lambda_d$, the ion and electron Larmor radii $\ell_i$ and $\ell_e$, the collisional mean-free-paths $\lambda_i$ and $\lambda_e$, and the plasma geometrical scale $R$.

This paper carries out a parametric study, based on asymptotic techniques, of a long cylindrical plasma confined by a strong axial magnetic field. This basic problem has been studied for many decades, producing a vast literature, which we will not attempt to summarize here. We will focus on works that, to our opinion, have been central on advancing on the understanding of the key physical phenomena and the characterization of the plasma response. It is quite evident that nowadays computational resources make immediate the numerical integration of the resulting steady-state equations for a 1D cylindrical magnetized plasma, no matter whether the selected model includes only the relevant phenomena or adds some extra ones that, at the end, turn out to be negligible. In this context, asymptotic and qualitative analyses continue to be especially useful since, first, they provide practical scaling laws and a clear and concise picture of the plasma response, and second, they guide in the formulation and treatment of more complex (two- and three-dimensional) problems.

[a)]Electronic mail: eduardo.ahedo@upm.es. Present address: E.T.S. Ingenieros Aeronáuticos, Plaza Cardenal Cisneros, Madrid 28040.

Tonks[1] presented an ambipolar diffusion theory for magnetic effects in a cylindrical plasma. As the magnetization strength decreases, his magnetized diffusive theory matches with the unmagnetized ambipolar diffusion theory of Schottky.[2] Tonks shows that, in the magnetized regime, electrons are confined by the magnetic field, and proposes for them a generalized form of the Boltzmann equilibrium law valid in the unmagnetized regime. The ambipolar diffusion theories of Schottky and Tonks are not applicable directly to a low-collisionality, small-Debye-length plasma, placed in front of a dielectric wall. In this case, an unmagnetized Debye sheath forms around the cylindrical wall, and a standard two-scale analysis separates the studies of the quasineutral plasma region and the non-neutral sheath. The sheath solution requires the fulfillment of the Bohm condition, which states that the ion flux at the sheath edge is not subsonic (in an appropriate sense).[3] Therefore, a correct matching at the sheath edge of the two regions implies that nonlinear ion inertia needs to be included in the model (as long as the Debye length is the smallest scale of the problem).

Ion inertia effects were considered by Forrest and Franklin[4] and Ewald *et al.*[5] The first ones kept a diffusive model for electrons but the second ones discussed also the relevance of electron inertia in the solution. Both works show that for high magnetization: ion-inertia effects tend to be limited to a thin layer near the sheath edge; the quasineutral solution matches with the Debye sheath when the ion velocity is equal to the simple sound velocity, independently of the magnetic strength; and a Tonks–Langmuir plasma balance equation[6] determines the plasma production frequency. Ewald *et al.*[5] achieve some additional results. First, they obtain analytical expressions for the plasma balance equation in the magnetized regime for both planar and cylindrical geom-

 

etries. Second, they find that the ion azimuthal drift (that is the macroscopic effect of the magnetic field on ions) is negligible in all practical regimes. Their last important conclusion (which is disputed in the present paper) is that electron inertia effects appear later than ion inertia effects and have a negligible effect in the solution.

The magnetized cylindrical problem, including electron inertia, has been revisited recently by Sternberg *et al.*,[7] who also provide a vast bibliographical review on the subject (although it does not include some of the central references). Sternberg *et al.* recover the main results of previous authors,[1,4,5] such as the scaling law for the production frequency of Ewald *et al.* Also, they assert that the electron azimuthal velocity approaches the electron thermal speed at the sheath edge, but they conclude that ignoring electron inertia has little effect on the numerical solution of the problem. They discuss in detail the expression for the ion resistivity, claiming it very relevant in the plasma response. The absence of the cylindrical terms in their momentum equations is a defect of their model, with consequences that will be commented below.

A central feature of the magnetized regime, which was implicit in Tonks' paper but has been highlighted by Sternberg *et al.*, is that the electron pressure gradient is balanced by the radial magnetic force, instead of by the electric force. As a consequence, electrons do not follow the Boltzmann equilibrium law. In a comment to their work, Allen[8] claims that the Boltzmann relation must hold in a vicinity of the Debye sheath edge, since the electric force dominates the magnetic force at the sheath edge. In their response, Sternberg *et al.*[9] replied that Allen's explanation is incorrect, invoking their results and the singular perturbation character of the plasma/sheath problem. In a later work on the subject, Allen[10] suggests that a more general "Boltzmann gradient condition" is satisfied at the edge rather than the Boltzmann condition itself.

Taking the works of Ewald *et al.* and Sternberg *et al.* as main references, this paper further analyzes the relevant physical phenomena, the spatial structure, and the parametric regimes of a cylindrical magnetized plasma. Among the new contributions that are presented for a magnetized plasma, we highlight that: (1) there are, indeed, two distinguished magnetized regimes when electron-collisionality is low; (2) there is no magnetized regime where electron azimuthal inertia is not relevant, contrary to previous authors' conclusions; (3) in the magnetized regimes, electron inertia effects cover a larger region than ion inertia ones; (4) Allen's claim on the dominance of the electric force near the sheath edge is correct; (5) the multiple-region structure of the plasma is discussed in detail; (6) the inner solution of the thin inertial layers are derived and provide the correct matching with the Debye sheath; and (7) simple scaling laws for plasma production and particle and energy fluxes to the wall are obtained.

Section II formulates the relevant plasma model starting from a model with full inertia terms for ions and electrons. Section III analyzes the different parametric regimes. Section IV discusses extensively the physical model and its results.

## II. MODEL FORMULATION

### A. Plasma equations

A plasma is confined by an axial magnetic field $\boldsymbol{B}=B1_z$ inside a long dielectric cylinder of radius $R$. The zero Debye length limit, $\lambda_D \ll$(rest of plasma lengths), is invoked, so that non-neutral effects are limited to a thin Debye sheath around the cylinder wall. This sheath is seen as a discontinuity in the quasineutral solution. Let points $O$ and $S$ represent the axis of the cylinder and the sheath edge, respectively. The plasma is stationary, axially symmetric ($\partial/\partial\theta=0$) and the derivatives with respect to $z$ are neglected formally. The macroscopic equations in the quasineutral region $OS$ are

$$\frac{1}{r}\frac{d}{dr}(rnu_r) = n\nu_w, \tag{1}$$

$$m_i u_r \frac{du_r}{dr} - m_i \frac{u_{\theta i}^2}{r} = -\frac{1}{n}\frac{d}{dr}(T_i n) - e\frac{d\phi}{dr} + eBu_{\theta i} - m_i(\nu_{in}+\nu_w)u_r, \tag{2}$$

$$m_e u_r \frac{du_r}{dr} - m_e \frac{u_{\theta e}^2}{r} = -\frac{1}{n}\frac{d}{dr}(T_e n) + e\frac{d\phi}{dr} - eBu_{\theta e} - m_e(\nu_{en}+\nu_w)u_r, \tag{3}$$

$$m_e u_r \frac{du_{\theta e}}{dr} + m_e \frac{u_{\theta e}u_r}{r} = eBu_r - m_e(\nu_{en}+\nu_w)u_{\theta e} - m_e\nu_{ei}(u_{\theta e}-u_{\theta i}), \tag{4}$$

$$m_i u_r \frac{du_{\theta i}}{dr} + m_i \frac{u_{\theta i}u_r}{r} = -eBu_r - m_i(\nu_{in}+\nu_w)u_{\theta i} + m_e\nu_{ei}(u_{\theta e}-u_{\theta i}). \tag{5}$$

Here most symbols are conventional. $\phi$ is the self-adjusted electric potential; $u_r=u_{re}=u_{ri}$ is the ambipolar radial velocity of both ions and electrons, consistent with a 1D model and a dielectric wall; $\nu_w$ is an effective frequency for volumetric production (that includes both ionization and axial diffusion); and $\nu_{en}$, $\nu_{in}$, and $\nu_{ei}$ represent binary collisions involving ions, electrons, and neutrals. The left-hand-sides of Eqs. (2)–(5) are the inertial terms, which consist of both gradient ($u_r d/dr$) and cylindrical ($\propto r^{-1}$) terms. The four cylindrical terms are missed by Sternberg *et al.*,[7] as Allen[10] already observed.

Several simplifications in Eqs. (1)–(5) are appropriate. First, the inertia gradient-term in the radial electron equation (3) is clearly negligible, but the inertia cylindrical-term, which involves $u_{\theta e}$, must be retained. Second, Ewald *et al.* found out that the ion azimuthal drift is negligible in all practical cases. Numerical evidence of it is also seen in Fig. 7 of Ref. 7. Analytical evidence is obtained from Eqs. (4) and (5) and $\nu_{in}, \nu_{en} \gg \nu_w, \nu_{ei}$; their diffusive limit yields $u_{\theta i}/u_{\theta e} \sim (m_e\nu_{in}/m_i\nu_{en})$; and for the case $\nu_{in}=\nu_{en}$ the exact solution of the full form of these two equations satisfies

$$u_{\theta i}(r) = u_{\theta e}(r) m_e/m_i.$$

Therefore, $u_{\theta i}$ can be dropped from the ion equations. Third, ion pressure will be dropped based on $T_i/T_e$ being small usually and the fact that it does not affect the qualitative plasma response (except for a small potential reversal at high magnetization[1]). Fourth, $T_e$ will taken constant, which is consistent with the large electron confinement and is supported by some experiments.[11] A more elaborate temperature model, based on solving the energy equation, presents the disadvantages of, first, complicating the parametric analysis and, second, being too dependent on the energy source model and the axial energy diffusion. Finally, all frequencies will be considered constant in our parametric study.

Next, in order to compare the terms involving $u_{\theta e}$ with the rest of terms, it is convenient to use the rescaled azimuthal velocity $u'_{\theta e}=u_{\theta e}\sqrt{m_e/m_i}$. Then, if $c_s=\sqrt{T_e/m_i}$ is the sound velocity, and $\omega_{lh}=eB(m_i m_e)^{-1/2}$ is the lower-hybrid frequency, the relevant form of Eqs. (2)–(4) is

$$u_r \frac{du_r}{dr} = -\frac{e}{m_i}\frac{d\phi}{dr} - \nu_i u_r, \tag{6}$$

$$0 = -c_s^2 \frac{d}{dr}(\ln n) + \frac{e}{m_i}\frac{d\phi}{dr} - \omega_{lh} u'_{\theta e} + \frac{u'^2_{\theta e}}{r}, \tag{7}$$

$$u_r \frac{du'_{\theta e}}{dr} = \omega_{lh} u_r - \nu_e u'_{\theta e} - \frac{u'_{\theta e} u_r}{r}, \tag{8}$$

with

$$\nu_e = \nu_{en} + \nu_{ei} + \nu_w, \quad \nu_i = \nu_{in} + \nu_w. \tag{9}$$

Equations (1), (6), and (7) lead to

$$\left(\frac{c_s^2}{u_r} - u_r\right)\frac{du_r}{dr} = \omega_{lh} u'_{\theta e} + \nu_i u_r + \nu_w \frac{c_s^2}{u_r} - \frac{u'^2_{\theta e} + c_s^2}{r}. \tag{10}$$

This equation shows that there is a turning point of the plasma profiles at $u_r=c_s$ that marks the entrance to the Debye sheath (and matches with the sonic Bohm condition required by the sheath solution). The two velocity components $u_r$ and $u'_{\theta e}$ are obtained from the integration of Eqs. (8) and (10). Then, Eqs. (6) and (7) determine $\ln n$ and $\phi$.

Boundary conditions at the cylinder axis $r=0$ are homogeneous,

$$u_r = u'_{\theta e} = u_{\theta i} = \phi = \ln(n/n_0) = 0, \tag{11}$$

with $n_0=n(0)$. Then, in order to start the numerical integration from the axis, it is necessary to use the Taylor expansion of the variables around $r=0$, which is of the form

$$(u_r, u'_{\theta e}, u_{\theta i}, e\phi/m_i, c_s^2 \ln n) \simeq (\nu_w/2)(r, a_2 r, -a_3 r, -a_4 r^2, -a_5 r^2), \tag{12}$$

where $a_2, \ldots, a_5$ are immediate to obtain. The integration must end at point $S$, $r=r_S \simeq R$, with

$$u_{rS} = c_s. \tag{13}$$

Dimensionless variables are defined using $T_e$ for energies, $c_s$ for velocities, $R$ for lengths, $n_0$ for the density, and the radial-transit frequency $c_s/R$ for the frequencies. Dimensionless variables are distinguished by a hat (e.g., $\hat{\omega}_{lh}=\omega_{lh}R/c_s$) with $\hat{u}_{\theta e}=u'_{\theta e}/c_s \equiv u_{\theta e}/c_e$ and $c_e=\sqrt{T_e/m_e}$ the electron thermal velocity. Thus, the relevant dimensionless model consists of

$$\left(\frac{1}{\hat{u}_r} - \hat{u}_r\right)\frac{d\hat{u}_r}{d\hat{r}} = \hat{\omega}_{lh}\hat{u}_{\theta e} + \hat{\nu}_i \hat{u}_r + \frac{\hat{\nu}_w}{\hat{u}_r} - \frac{1}{\hat{r}} - \frac{\hat{u}^2_{\theta e}}{\hat{r}}, \tag{14}$$

$$\hat{u}_r \frac{d\hat{u}_{\theta e}}{d\hat{r}} = \hat{\omega}_{lh}\hat{u}_r - \hat{\nu}_e \hat{u}_{\theta e} - \frac{\hat{u}_{\theta e}\hat{u}_r}{\hat{r}}, \tag{15}$$

$$0 = -\frac{d\ln\hat{n}}{d\hat{r}} + \frac{d\hat{\phi}}{d\hat{r}} - \hat{\omega}_{lh}\hat{u}_{\theta e} + \frac{\hat{u}^2_{\theta e}}{\hat{r}}, \tag{16}$$

$$\frac{d\hat{\phi}}{d\hat{r}} = -\hat{u}_r \frac{d\hat{u}_r}{d\hat{r}} - \hat{\nu}_i \hat{u}_r. \tag{17}$$

Equations (14)–(17) have $\hat{\nu}_w$ as eigenvalue, and three free dimensionless parameters: $\hat{\omega}_{lh}$, $\hat{\nu}_e$, and $\hat{\nu}_i$. The fulfillment at the sheath edge of the extra condition (13) determines the plasma balance equation[4–6] for the eigenvalue $\hat{\nu}_w$ in the form

$$\hat{\nu}_w = \hat{\nu}_w(\hat{\omega}_{lh}, \hat{\nu}_e, \hat{\nu}_i), \tag{18}$$

or taking into account that $\hat{\nu}_w$ is also part of $\hat{\nu}_e$ and $\hat{\nu}_i$, Eq. (9),

$$\hat{\nu}_w = \hat{\nu}_w(\hat{\omega}_{lh}, \hat{\nu}_{en} + \hat{\nu}_{ei}, \hat{\nu}_{in}). \tag{19}$$

The dimensionless frequencies in this relation represent length ratios too,

$$\hat{\omega}_{lh} = R/\ell_e, \quad \hat{\nu}_{en} + \hat{\nu}_{ei} = (m_i/m_e)^{1/2} R(\lambda_{en}^{-1} + \lambda_{ei}^{-1}),$$

$$\hat{\nu}_{in} = R/\lambda_{in},$$

where $\ell_e=c_s/\omega_{lh}$ is the electron (thermal) gyroradius, and the $\lambda$'s are collisional mean-free-paths. Equation (19) states that the plasma response of the relevant model, Eqs. (14)–(17), depends on three parameters relating the magnetic strength ($\omega_{lh}$), the electron collisionality with ions plus neutrals ($\nu_{en}+\nu_{ei}$), the ion-neutral collisionality ($\nu_{in}$), and the radial transit time ($R/c_s$). Furthermore, the normalized equations (14)–(17) suggest that for $\hat{\omega}_{lh}, \hat{\nu}_e, \hat{\nu}_i = O(1)$ (that is, for intermediate magnetization and collisionality) all terms in the equations are of the same order and $\hat{\nu}_w = O(1)$. In particular, this means that electron inertia terms, which consist of the double contribution $(\hat{u}_r/\hat{r})d(\hat{r}\hat{u}_{\theta e})/d\hat{r}$ to the azimuthal equation (15) and the cylindrical term in the radial equation (16), are non-negligible. These provisional conclusions on the plasma response already mean an advance with respect to the original model, Eqs. (1)–(5), which just stated that the response could depend on two more parameters: $\sqrt{m_e/m_i}$ and say, $\hat{\nu}_{ei}$.

The main output parameters of the problem are the production frequency $\hat{\nu}_w$ and the fluxes of particles and energy to the sheath and wall. It can be said that the production frequency determines either $T_e$ (if there is no axial diffusion) or the axial particle diffusion (if $T_e$ is obtained from the axial response). The ion/electron flux to the Debye sheath and wall is $n_S c_s$. Thus, the dimensionless parameter $\hat{n}_S$ measures both the density at the sheath edge $S$ and the particle flux to sheath and wall $W$. The flux of plasma energy into sheath and wall is $E_W n_S c_s$, where the energy deposited by unit of plasma flux is

$$E_W = \frac{T_e}{2} + T_e \ln\sqrt{\frac{m_i}{2\pi m_e}} + 2T_e + \frac{m_e u_{\theta eS}^2}{2}. \tag{20}$$

Here, on the right-hand side, the terms from left to right are the following: the ion kinetic energy at the sheath edge $S$, the energy exchanged between ions and electrons inside the zero-current sheath, and the internal and directed azimuthal energies deposited at the wall per collected electron. A near Maxwellian distribution function with an azimuthal drift $u_{\theta eS}$ has been considered for the confined electron population.

## III. PLASMA REGIMES AND QUASINEUTRAL REGIONS

Three plasma regimes are identified in the parametric space $(\hat{\omega}_{lh}, \hat{\nu}_e, \hat{\nu}_i)$. (In general, $\hat{\nu}_e$ and $\hat{\nu}_i$ are more convenient for the analysis than $\hat{\nu}_{en}+\hat{\nu}_{ei}$ and $\hat{\nu}_{in}$.)

### A. The main magnetized regime

Let us consider first the parametric domain

$$\hat{\omega}_{lh} \gg 1, \quad \hat{\nu}_e, \hat{\nu}_i = O(1). \tag{21}$$

It will be found that $\hat{\nu}_w \ll 1$, so that $\hat{\nu}_i \simeq \hat{\nu}_{in}$ and $\hat{\nu}_e \simeq \hat{\nu}_{en} + \hat{\nu}_{ei}$. A two-region quasineutral structure, consisting of a diffusive bulk region followed by a thin layer with steepened profiles has been observed.[4,5]

Two-scale studies of magnetized plasma models comparable to the present one[12–14] suggest the procedure to follow here. The plasma behavior in the bulk region comes out from dropping the inertia terms in Eqs. (14)–(16) and neglecting the electric field in Eq. (16). This leads to the diffusive solution[1]

$$\hat{u}_r = \frac{\hat{\nu}_e}{\hat{\omega}_{lh}}\hat{u}_{\theta e}, \tag{22}$$

$$\hat{\omega}_{lh}\hat{u}_{\theta e} = -\frac{d\ln\hat{n}}{d\hat{r}}, \tag{23}$$

$$\frac{d^2\hat{n}}{d\hat{r}^2} + \frac{1}{\hat{r}}\frac{d\hat{n}}{d\hat{r}} + a_0^2\hat{n} = 0, \tag{24}$$

with

$$a_0 = \hat{\omega}_{lh}\sqrt{\hat{\nu}_w/\hat{\nu}_e}. \tag{25}$$

The solution is[1,5]

$$\hat{n}(\hat{r}) = J_0(a_0\hat{r}),$$
$$\hat{u}_r(\hat{r}) = \frac{\hat{\nu}_e}{\hat{\omega}_{lh}}\hat{u}_{\theta e} = a_0\frac{\hat{\nu}_e}{\hat{\omega}_{lh}^2}\frac{J_1(a_0\hat{r})}{J_0(a_0\hat{r})}, \tag{26}$$

with $J_0$ and $J_1$ Bessel functions of the first kind.

The diffusive solution is valid until one of the inertia (gradient-)terms in Eqs. (14) and (15) becomes of dominant order. The electron equation (15) has $d\hat{u}_{\theta e}/d\hat{r} \sim \hat{\omega}_{lh}$ for $\hat{u}_{\theta e} \sim 1$. This means $\hat{u}_r \sim \hat{\nu}_e/\hat{\omega}_{lh}$ and the inertial term on the ion equation (14) is still small. Therefore, the transition to an inertial region is marked by the appearance of electron inertia and *not* by ion inertia, as Ewald *et al.* asserted.

The (regular) transition to the inertial layer can be located at the electron sonic point $D$, defined as $\hat{u}_{\theta eD}=1$, where $\hat{u}_{rD} \sim \hat{\nu}_e/\hat{\omega}_{lh}$. Then, if the inertial layer is assumed thin, its relevant equations come out from dropping the cylindrical, collisional, and production terms from Eqs. (14)–(17), and the solution for the velocty field in the inertial layer is

$$\hat{u}_{\theta e} = \hat{\omega}_{lh}(\hat{r}-\hat{r}_D) + b_1,$$
$$2\ln\frac{\hat{u}_r\hat{\omega}_{lh}}{\hat{\nu}_e} - \hat{u}_r^2 = \hat{\omega}_{lh}^2(\hat{r}-\hat{r}_D)^2 + 2b_1\hat{\omega}_{lh}(\hat{r}-\hat{r}_D) + b_2, \tag{27}$$

with $b_1$ and $b_2$ constants of $O(1)$ that assure the gentle matching of the bulk and inertial regions around point $D$. Profiles of $\hat{\phi}$ and $\hat{n}$ in the inertial layer are obtained from

$$\hat{\phi} + \hat{u}_r^2/2 = \text{const}, \quad \hat{n}\hat{u}_r = \text{const}. \tag{28}$$

Setting $\hat{u}_{rS}=1$ in Eq. (27), allows us to estimate both the thickness of the inertial layer $d$ and the electron azimuthal drift at the sheath edge. One finds

$$d \sim \ell_e\sqrt{2\ln\frac{\hat{\omega}_{lh}}{\hat{\nu}_e}}, \tag{29}$$

$$\hat{u}_{\theta eS} \simeq \sqrt{2\ln\frac{\hat{\omega}_{lh}}{\hat{\nu}_e}} - 0.5, \tag{30}$$

where the last term in Eq. (30) has been adjusted using the exact numerical solution. Therefore, both $d/\ell_e$ and $u_{\theta eS}/c_e$ are logarithmically large, whereas $d/R \sim \hat{\omega}_{lh}^{-1}\hat{u}_{\theta eS}$ is still small, as anticipated. Second, ion inertia effects are of dominant order *only within* an ion-inertial sublayer next to the sheath edge $S$ of thickness $d_i$, satisfying

$$d_i \sim \ell_e\hat{u}_{\theta eS}^{-1} \ll d \sim \ell_e\hat{u}_{\theta eS}. \tag{31}$$

The velocity field in the ion-inertial sublayer satisfies

$$\hat{u}_{\theta e} \simeq \hat{u}_{\theta eS},$$
$$\ln\hat{u}_r + (1-\hat{u}_r^2)/2 = -\hat{\omega}_{lh}\hat{u}_{\theta eS}(1-\hat{r}). \tag{32}$$

Once the inertial layer has been confirmed to be thin, setting $\hat{r}_D \simeq 1$ and $\hat{u}_{\theta eD}=1$ in Eq. (26) yields that, up to dominant order, $a_0$ must be the first-zero of $J_0$, i.e., $a_0 \simeq 2.405$. Therefore, Eq. (25) yields the plasma balance equation for this regime,[5]

$$\hat{\nu}_w(\hat{\omega}_{lh}, \hat{\nu}_e) = a_0^2 \hat{\nu}_e / \hat{\omega}_{lh}^2, \tag{33}$$

$a_0^2 \simeq 5.78$. The plasma flow in the bulk region satisfies

$$2\pi \hat{r} \hat{n} \hat{u}_r = 2\pi \hat{\nu}_w J_1(a_0 \hat{r})/a_0, \tag{34}$$

and is constant in the (thin) inertial and Debye layers. Thus, the particle flux to the wall, is the particle flux at $D$, which is $(\hat{n}\hat{u}_r)_W = \hat{\nu}_w J_1(a_0)/a_0$. In dimensionless form, this flux is[7]

$$\hat{n}_S(\hat{\omega}_{lh}, \hat{\nu}_e) = a_0 J_1(a_0)\, \hat{\nu}_e / \hat{\omega}_{lh}^2, \tag{35}$$

which is also the plasma density at point $S$; $a_0 J_1(a_0) \simeq 1.25$. The plasma density at point D is $\hat{n}_D = \hat{n}_S / \hat{u}_{rD} \sim a_0 J_1(a_0)/\hat{\omega}_{lh}$.

Figures 1 and 2 compare exact numerical solutions and asymptotic ones for several $\hat{\nu}_{in}$ and $\hat{\nu}_{e(n+i)} \equiv \hat{\nu}_{en} + \hat{\nu}_{ei}$. Figure 1 shows the formation of the thin inertial layer as the magnetic strength $\hat{\omega}_{lh}$ increases and confirms the validity of the above asymptotic analysis. Observe, in Fig. 1(a) how point $D$ is located at the knee of $\hat{u}_r(\hat{r})$ and in Fig. 1(d), how the profiles of $\hat{n}(\hat{r})$ tend to Eq. (26) when $\hat{\omega}_{lh}/\hat{\nu}_e \to \infty$. Figure 2 shows the dependence of main plasma parameters on $\hat{\omega}_{lh}$ and $\hat{\nu}_{en} + \hat{\nu}_{ei}$, and the validity of the above asymptotic scaling laws for strong magnetization.

From Eq. (17) the (negative) potential fall in the bulk region is

$$-\hat{\phi}_D \sim \frac{\nu_e}{\omega_{lh}} \max\left\{\frac{\nu_i R}{c_s}, \frac{\nu_e}{\omega_{lh}}\right\} \ll 1, \tag{36}$$

and amounts to $\hat{\phi}_D - \hat{\phi}_S \simeq -1/2$ in the inertial layer. Interestingly, the electric force makes a negligible contribution to the electron balance in Eq. (16) except within the ion-inertial sublayer. In that sublayer

$$\frac{d\hat{\phi}}{d\hat{r}} \simeq -\frac{\hat{u}_r^2}{1-\hat{u}_r^2} \hat{\omega}_{lh} \hat{u}_{\theta eS}, \tag{37}$$

so that $|d\hat{\phi}/d\hat{r}| > \hat{\omega}_{lh}\hat{u}_{\theta e}$ for $\hat{u}_r^2 > 1/2$. Therefore, near the sheath edge the electric force dominates over the magnetic force and Eq. (16) reduces to the Boltzmann relation.

Finally, we remind that, at high magnetization, (small) ion pressure effects can reverse the potential profile in the bulk region, creating a small bump.[1] Adding the term $-(T_i/T_e) d \ln \hat{n}/d\hat{r}$ to the right-hand side of Eq. (17), the potential profile in the bulk region satisfies

$$\hat{\phi} = \left(\frac{\nu_i \nu_e}{\omega_{lh}^2} - \frac{T_i}{T_e}\right) \ln \hat{n} - \frac{\hat{u}_r^2}{2}. \tag{38}$$

Therefore, if

$$1 \gg \frac{T_i}{T_e} \gg \frac{\nu_e}{\omega_{lh}} \max\left\{\frac{\nu_i R}{c_s}, \frac{\nu_e}{\omega_{lh}}\right\}, \tag{39}$$

the reverse potential profile in the diffusive region is $\Delta\hat{\phi} \sim \hat{T}_i \hat{\omega}_{lh}$. Observe that Eq. (38) is valid for both the bulk region and the inertial layer; it adds ion inertia to the purely diffusive expression of Tonks. Since the electric potential is a second order contribution ($\hat{\phi} \ll \ln \hat{n}$), the inclusion of the small ion pressure does not modify the plasma balance equation (33).

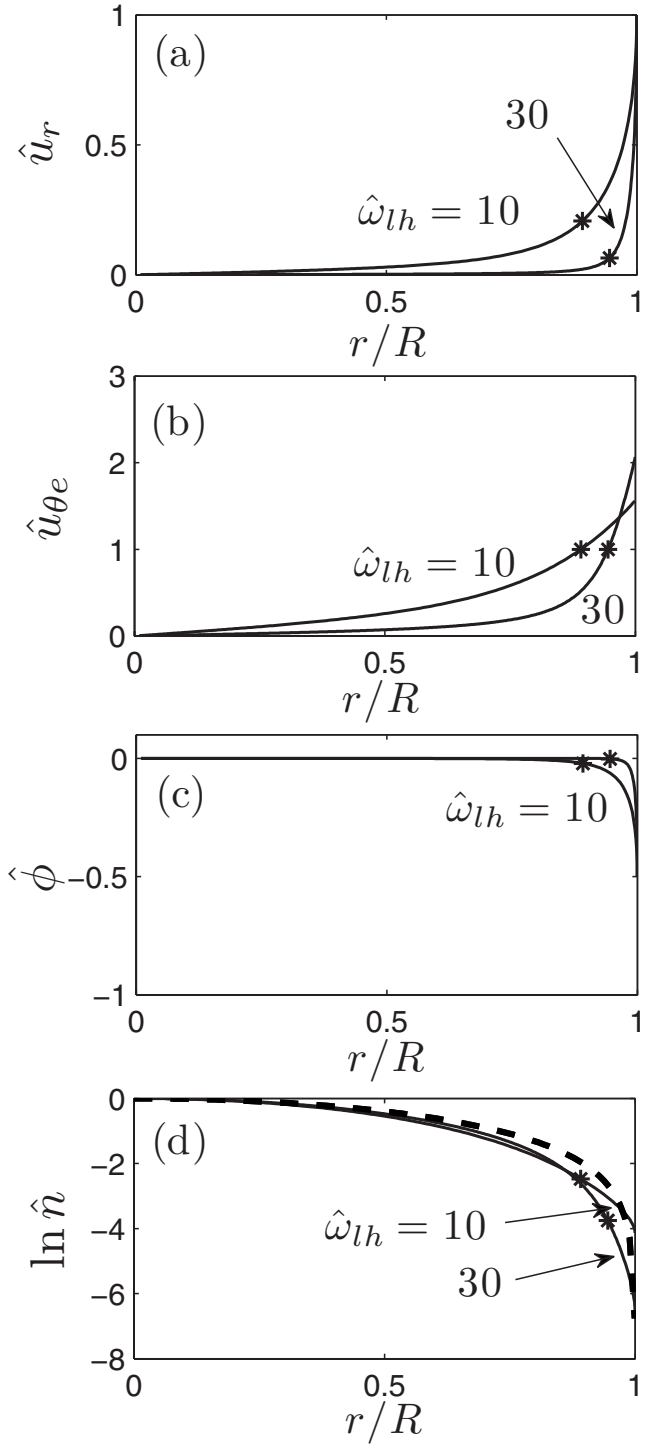


FIG. 1. Plasma profiles for $\hat{\omega}_{lh} = 10$, and 30; $\hat{\nu}_{in} = 0$ and $\hat{\nu}_{e(n+i)} \equiv \nu_{en} + \nu_{ei} = 1$. The asterisks correspond to location of point $D$, where the electron azimuthal velocity becomes comparable with the electron thermal velocity. The dashed line in (d) corresponds to the asymptotic solution (26) for $\omega_{lh}/\nu_e \to \infty$.

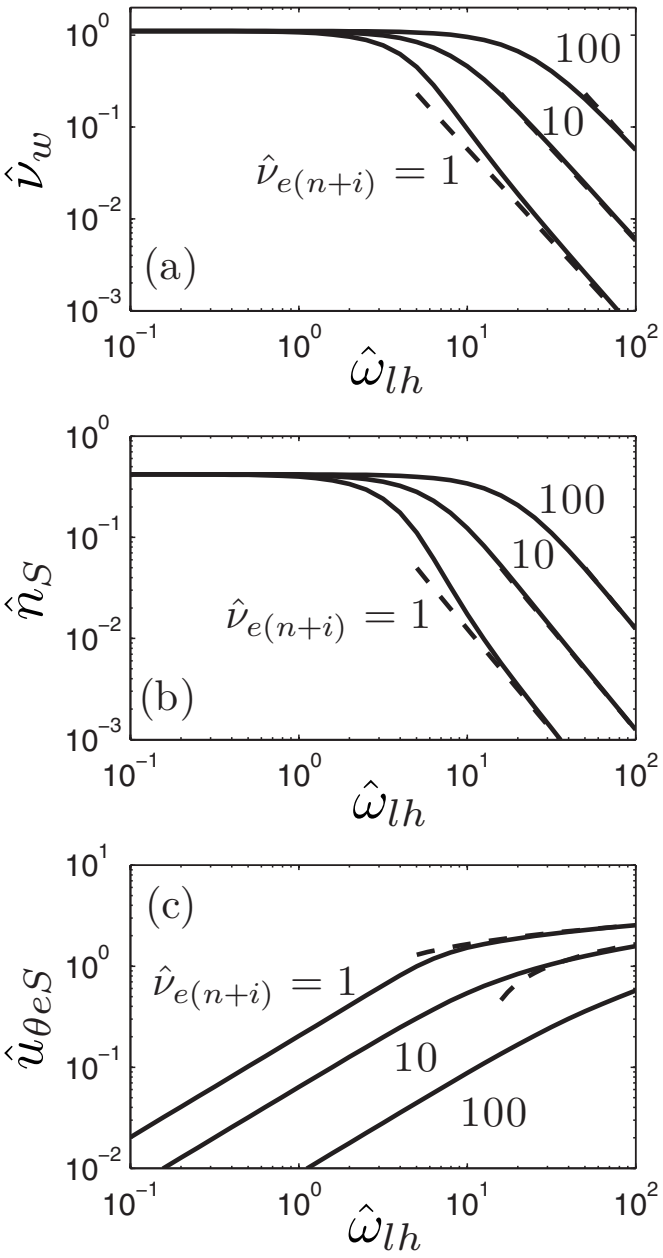


FIG. 2. Plasma parameters for $\hat{\nu}_{e(n+i)}=1$, 10, and 100; $\hat{\nu}_{in}=0$. Dashed lines correspond to the asymptotic laws (33) and (35) of the magnetized regime.

### B. The unmagnetized regime

In order to determine the boundaries of the magnetized regimes, the plasma response in the unmagnetized regime (UR), studied by Self and Ewald,[15] is briefly characterized. For $\hat{\omega}_{lh}\ll 1$, $\hat{u}_{\theta e}$ becomes small and can be dropped from Eqs. (14) and (16). Then, both $\hat{\omega}_{lh}$ and $\hat{\nu}_e$ disappear from the main model, and $\hat{\nu}_{in}$ remains the only parameter of the UR, where ion-collisionless and ion-collisional subregimes, $\hat{\nu}_{in}\ll 1$ and $\hat{\nu}_{in}\gg 1$, respectively, are to be distinguished.

In the ion-collisionless limit $\hat{\nu}_{in}\to 0$, the numerical integration yields

$$\hat{n}_S \simeq 0.42, \quad \hat{\nu}_w = \hat{\nu}_{w0} \simeq 1.11. \tag{40}$$

In the ion-collisional regime (where $\nu_i \simeq \nu_{in}$), the unmagnetized plasma presents again a two-region structure, consisting of a bulk diffusive region and a thin inertial layer, governed by ion inertia, with a transition at $\hat{u}_r \sim \hat{\nu}_{in}^{-1/2}$. The solution in the diffusive region for $\hat{n}$ and $\hat{u}_r$ is formally identical to the solution of the diffusive region of the magnetized regime (MR) by just exchanging $\hat{\omega}_{lh}^2/\hat{\nu}_e$ by $\hat{\nu}_{in}$.[1,5] Thus, the spatial response is

$$\hat{n} = J_0(a_0\hat{r}), \quad \hat{u}_r = \frac{a_0}{\hat{\nu}_{in}}\frac{J_1(a_0\hat{r})}{J_0(a_0\hat{r})}, \tag{41}$$

and the production frequency and flux to wall are

$$\hat{\nu}_w(\hat{\nu}_{in}) = \frac{a_0^2}{\hat{\nu}_{in}}, \quad \hat{n}_S(\hat{\nu}_{in}) = \frac{a_0 J_1(a_0)}{\hat{\nu}_{in}}. \tag{42}$$

Then, the inertial layer has a thickness $O(\hat{\nu}_{in}^{-1/2})$ and inside it, $\hat{u}_r(\hat{r})$ satisfies $\hat{u}_r+\hat{u}_r^{-1}+\hat{\nu}_{in}(1-\hat{r})\approx\hat{\nu}_{in}$.

The influence of $\hat{\nu}_{in}$ in the production frequency $\hat{\nu}_w$ is illustrated in Fig. 3. Together, Figs. 2 and 3 illustrate well the three-parameter, plasma balance condition $\hat{\nu}_w(\hat{\omega}_{lh},\hat{\nu}_e,\hat{\nu}_{in})$ for $\hat{\nu}_e \geq O(1)$, any $\hat{\nu}_{in}$ and any $\hat{\omega}_{lh}$ (i.e., from the unmagnetized to the magnetized regime). Notice that in the region where $\hat{\nu}_w$ depends on $\hat{\nu}_e$, it is $\hat{\nu}_e \simeq \hat{\nu}_{en}+\hat{\nu}_{ei}$.

### C. The collisionless, intermediate-magnetization regime

The preceding two regimes do not cover the case of intermediate magnetization for a near-collisionless plasma. In order to complete the regime characterization, we consider the parametric region

$$\hat{\omega}_{lh} \gg 1, \quad \hat{\nu}_{in}\to 0, \quad \hat{\nu}_{en}+\hat{\nu}_{ei}\to 0, \tag{43}$$

and $\hat{\nu}_w \ll 1$ is expected. For this electron-collisionless plasma, dropping $\hat{\nu}_e$ and $\hat{\nu}_i$ in Eqs. (14)–(17) yields, first,

$$\hat{u}_{\theta e} = \hat{\omega}_{lh}\hat{r}/2, \tag{44}$$

then,

$$\ln\hat{n} + \frac{\hat{u}_r^2}{2} + \frac{\hat{\omega}_{lh}^2}{8}\hat{r}^2 = 0, \tag{45}$$

$$\hat{\phi} + \frac{\hat{u}_r^2}{2} = 0, \tag{46}$$

and, finally,

$$\left(\frac{1}{\hat{u}_r}-\hat{u}_r\right)\frac{d\hat{u}_r}{d\hat{r}} = \frac{\hat{\omega}_{lh}^2}{4}\hat{r} + \frac{\hat{\nu}_w}{\hat{u}_r} - \frac{1}{\hat{r}}. \tag{47}$$

The solution of this last equation is

$$\hat{u}_r \simeq \hat{\nu}_w\hat{r}/2, \tag{48}$$

for $\hat{r}\ll\hat{\omega}_{lh}^{-1}$, and

$$\frac{\hat{u}_r^2}{2} - \ln(\hat{r}\hat{u}_r) + \frac{\hat{\omega}_{lh}^2}{8}\hat{r}^2 = \text{const} = \frac{1}{2} + \frac{\hat{\omega}_{lh}^2}{8} = \ln\frac{\hat{\omega}_{lh}^2}{4\hat{\nu}_w}, \tag{49}$$

for $\hat{\omega}_{lh}^{-1}\ll\hat{r}\leq 1$. The constant on the right-hand side of Eq. (49) has been obtained from both the matching with Eq. (48) at $\hat{r}=O(\hat{\omega}_{lh}^{-1})$ and the sonic condition at $S$. The two values of the constant yield the law for the plasma production,

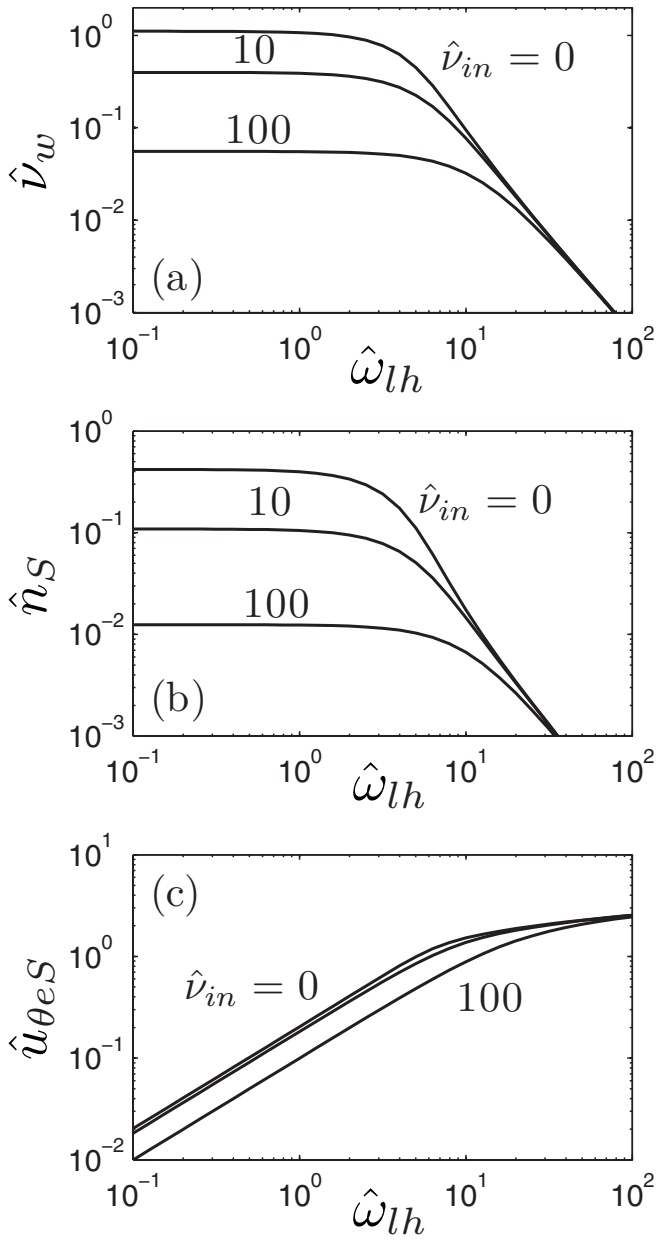


FIG. 3. Plasma parameters for $\hat{\nu}_{in}=0$, 10, and 100; $\hat{\nu}_{e(n+i)}=1$. Asymptotic laws (42) apply for $\hat{\omega}_{lh}$ small.

$$\hat{\nu}_w(\hat{\omega}_{lh}) = \frac{\hat{\omega}_{lh}^2}{4}\exp\left(-\frac{1}{2}-\frac{\hat{\omega}_{lh}^2}{8}\right), \tag{50}$$

and Eq. (45) yields the plasma flux,

$$\hat{n}_S(\hat{\omega}_{lh}) = \exp\left(-\frac{1}{2}-\frac{\hat{\omega}_{lh}^2}{8}\right). \tag{51}$$

Figure 4 depicts this intermediate-magnetization regime (IR), which is located between the unmagnetized and the main magnetized regimes, UR and MR. The dashed lines correspond to the asymptotic solution for a collisionless plasma (including the approximation $\hat{\nu}_w=0$). This distinguished collisionless magnetized regime exists as long as $\hat{\nu}_e \ll 1$ and $\hat{\nu}_{in} \leq O(1)$.

The solution (44) shows that the azimuthal electron velocity is governed fully by electron inertia (with the gradient and cylindrical terms having the same weight) *in the whole plasma region*, i.e., $0 \leq \hat{r} \leq 1$. From solution (49), ion inertia is significant only in a thin inertial layer of thickness $d_i \sim \ell_e$. Equations (45) and (46) show that the electric field is negligible except in the ion inertial layer, and again electrons recover the Boltzmann relation in the vicinity of the sheath edge.

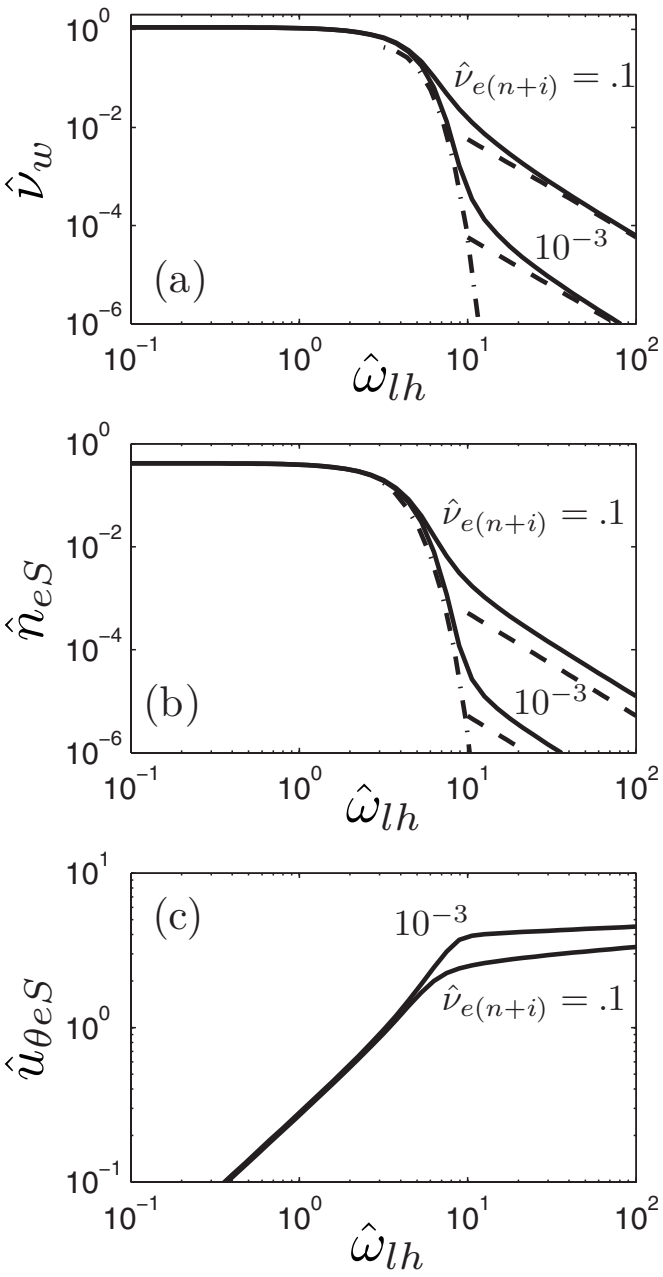


FIG. 4. Plasma parameters for $\hat{\nu}_{e(n+i)}=10^{-3}$ and $10^{-1}$; $\hat{\nu}_{in}=0$. Dashed lines correspond to the asymptotic laws (33) and (35) of the MR. Dash-and-dot lines correspond to the asymptotic laws (50) and (51) of the collisionless IR.

### D. Summary of regimes

The preceding study has characterized completely the plasma regimes covering the whole parametric space $(\hat{\omega}_{lh}, \hat{\nu}_e, \hat{\nu}_{in})$, with $\hat{\nu}_e \simeq \hat{\nu}_{en}+\hat{\nu}_{ei}$. There is (a) the UR, where the plasma response depends only on ion collisionality, $\hat{\nu}_{in}$, (b) the MR, where the response depends only on the "per-

pendicular transport frequency," $\hat{\omega}_{lh}^2/\hat{\nu}_e$, and (c) the IR, which exists only for low electron-collisionality and, to our knowledge, had not been identified previously in theoretical studies.

For moderate and high electron collisionality (i.e., $\hat{\nu}_e$ large), the patched expression

$$\hat{\nu}_w = \frac{a_0^2 \hat{\nu}_{w0}}{a_0^2 + \hat{\nu}_{w0}(\hat{\nu}_{in} + \hat{\omega}_{lh}^2/\hat{\nu}_e)}, \tag{52}$$

is a good approximation of the plasma balance equation for any $\hat{\omega}_{lh}$ and $\hat{\nu}_{in}$; for $\hat{\nu}_e \sim 2-50$, the maximum error of that expression [at $\hat{\omega}_{lh}=O(1)$] is $\sim \hat{\nu}_e^{-1}$. The transition between the UR and the MR takes place around $\hat{\omega}_{lh} \sim \sqrt{\hat{\nu}_{in}\hat{\nu}_e}$, as Figs. 2 and 3 illustrate.

For low-electron collisionality [and $\hat{\nu}_{in} \leq O(1)$] the transitions of the IR with the UR and MR are located at $\hat{\omega}_{lh} \sim 1$ and $\hat{\omega}_{lh}^4 \exp(-\hat{\omega}_{lh}^2/8) \sim \hat{\nu}_e$, respectively. Low-electron collisionality is more common for a low-density, hot, fully ionized plasma; for instance, one has $\hat{\nu}_e \approx 10^{-2}$ for argon, $R=1$ cm, $n_e=10^{-16}$ m$^{-3}$, and $T_e=17$ eV.

## IV. DISCUSSION

### A. The role of electron inertia

Ewald *et al.* claimed that electron inertia effects were negligible in the plasma solution. More recently, Sternberg *et al.* grant only a minor role to electron inertia. Our study, carried out essentially on the same physical model, reaches a very different conclusion: there is no magnetized regime where electron inertia is not relevant or even has a lesser role than ion inertia. To support this, our asymptotic analysis reveals the details of the structure of the quasineutral plasma in the two magnetized regimes.

In the MR, there is a bulk diffusive region and a thin inertial layer governed mainly by electron (azimuthal) inertia. Ion (radial) inertia becomes dominant only within a thinner sublayer, adjacent to the Debye sheath edge. In the MR, both the production frequency and the particle flux to the wall can be obtained from the solution of the diffusive region.[5] This could lead to the wrong impression that the inertial layer and electron inertia are marginal in the solution. The inner solution of the inertial layer of the MR is important because it provides, first, the correct matching with the Debye sheath and, second, the correct electron azimuthal energy at point $S$ with its dependence on $\ln(\omega_{lh}/\nu_e)$. The directed electron energy (which can be deposited at the walls) turns out to be larger than the thermal energy, Eq. (30), and a major part of it is acquired within the (electron) inertial layer.

In the IR, there is not a purely diffusive region. Electron azimuthal inertia is relevant in the whole bulk region, whereas ion inertia effects are reduced to a thin layer near the sheath edge. As a consequence, in this regime, plasma production and flux to the wall are affected by electron inertia but not by ion inertia. [In the UR, electron inertia effects become negligible and a thin ion-inertial layer appears only in the ion-collisional limit.]

The different behaviors of the electron azimuthal velocity merit further discussion. Equation (15) can be written as

$$\frac{\hat{u}_r}{\hat{r}}\frac{d(\hat{r}\hat{u}_{\theta e})}{d\hat{r}} + \hat{\nu}_e \hat{u}_{\theta e} = \hat{\omega}_{lh}\hat{u}_r,$$

and shows that the (varying) driving force $\hat{\omega}_{lh}\hat{u}_r$ generates $\hat{u}_{\theta e}$ through the first, inertial term on the left-hand side, whereas the second, resistive term saturates the growth of $\hat{u}_{\theta e}$. For a low electron-collisionality plasma, the competition between the two terms on the left-hand side explains the different behaviors in the IR and the MR: in the IR (and the UR) $\hat{u}_{\theta e}$ does not saturate, Eq. (44); in the bulk region of the MR, $\hat{u}_{\theta e}$ saturates at any point with the local value of $\hat{\omega}_{lh}\hat{u}_r$, Eq. (22); and, in the inertial layer of the MR, $\hat{u}_{\theta e}$ does not saturate because of the strong gradient of the driving force.

In the MR, $\hat{u}_{\theta e}$ is indeed a $\nabla p \times \boldsymbol{B}$ drift up to the ion-inertial sublayer. More precisely, one has

$$u_{\theta e} \simeq -\frac{1}{eB}\frac{\partial H_e}{\partial r},$$

with $H_e = T_e \ln(n/n_0)$ the electron enthalpy. Inside the inertial layer, the radial changes in electron enthalpy $\Delta H_e \simeq T_e \ln(n_S/n_D)$ are much larger than $T_e$ and the effective magnetic length for the electron fluid is

$$\ell_e^* = \frac{m_e}{eB}\sqrt{\frac{\Delta H_e}{m_e}} = \ell_e \sqrt{\frac{\Delta H_e}{T_e}}, \tag{53}$$

which is larger than the electron (thermal) gyroradius, and can be interpreted as an effective electron gyroradius. This explains that the thickness of the inertial layer is $d \sim \sqrt{2}\ell_e^*$, Eq. (29).

An inertial layer governed by the electron azimuthal drift and a thickness proportional to an effective electron gyroradius was found by Ahedo and Escobar[13] for a problem with a wall-parallel magnetic field, but different geometry and a conducting wall. On the contrary, the inertial layer in comparable models with an *oblique* magnetic field (and Boltzmann equilibrium for electrons)[12,16,17] is governed by the ion azimuthal drift and its thickness is proportional to an effective ion gyroradius. This is true even in the "near-parallel" case, as long as electrons are still in Boltzmann equilibrium.[14]

In a cylindrical geometry, inertial terms consists of both gradient and cylindrical terms, and these last ones can be of dominant order for electrons. For instance, in the radial direction, Eq. (3), the centrifugal term $m_e u_{\theta e}^2/r$ can be relevant whereas $m_e du_r/dr$ is negligible always. Sternberg *et al.* ignore totally cylindrical terms in the momentum equations (but not in their continuity equation). This is a serious flaw in the IR, where the two electron cylindrical terms are of dominant order. To illustrate it, Fig. 5 shows the relative errors committed in the plasma flux and the electron azimuthal current at the wall, when cylindrical terms are dropped from the equations. The azimuthal electron drift, Fig. 5(b), is overestimated by a factor up to 2, but the plasma flux to the wall, Fig. 5(a), and the production frequency can be underestimated by one order of magnitude. The explanation of such large errors is the following. The error in $\hat{u}_{\theta e}$ is due to the gradient and cylindrical terms being similar in Eq. (15), as the solution (44) shows. A change by a factor of 2 in $\hat{u}_{\theta e}$

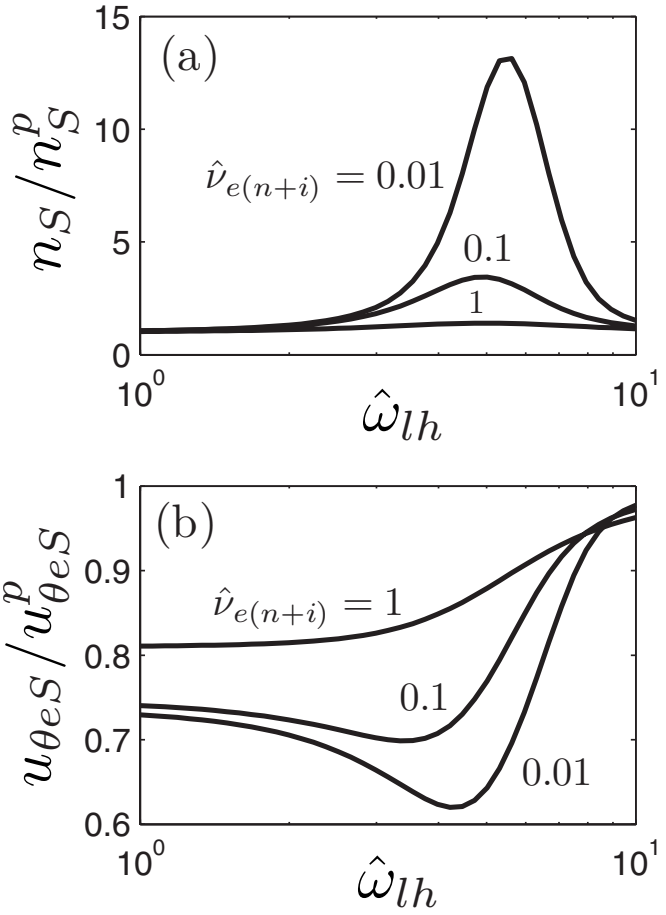


FIG. 5. Relative errors when electron cylindrical terms are dropped from the model, for $\hat{\nu}_{e(n+i)}=0.01$, 0.1, and 1; $\hat{\nu}_{in}=0$. Superscript $p$ corresponds to "planarlike" momentum equations.

implies to exchange $\hat{\omega}_{lh}^2$ by $\hat{\omega}_{lh}^2/4$ in Eq. (47); then, this change is transferred to the exponential terms of the scaling laws (50) and (51). Electron cylindrical terms do not play any role in the UR, where $\hat{u}_{\theta e}$ is negligible, and they are small compared with the gradient terms in the MR.

The preceding discussion suggests differences in the solutions for the planar and cylindrical versions of the present problem. The equations for the two cases differ only in the cylindrical terms in the continuity and momentum equations. In the continuity equation and for $\hat{r} \ll 1$, one has $\hat{u}_r \simeq \hat{r}\hat{\nu}_w/2$ and $\hat{u}_r \simeq \hat{r}\hat{\nu}_w$ for the cylindrical and planar cases, respectively, but the relevance of the cylindrical terms on the electron momentum equations reveals that the production frequency in the planar case of the IR is going to be much smaller than in the present cylindrical case.

### B. Force and energy balances

In the UR the electron pressure gradient is compensated by the electric force, which implies that electrons follow the Boltzmann equilibrium law. On the contrary, in the MR, the pressure gradient is balanced by the magnetic force up to the ion-inertial sublayer. In the IR, the electron centrifugal force is of the same order than the pressure gradient, Eq. (16), and both need to be balanced by the magnetic force. The magnetic confinement produces a strong concentration of the plasma around the axis; two-orders of magnitude of radial decay in the plasma density have been measured in recent experiments.[11,18] If ion collisionality is small, the potential fall in the quasineutral plasma is similar in the unmagnetized and magnetized regimes, but it is concentrated near the sheath edge in the magnetized regime.

Differences in the force balance between the unmagnetized and magnetized regimes are more modest for ions than for electrons. In all regimes the ambipolar electric field drives the ion radial acceleration, Eq. (17); in addition, it might have to compensate the ion resistivity in the UR and the ion pressure in the MR. The different role of the electric field for electrons and ions in the bulk regions of the magnetized regimes indicates that the terms involved in the ion radial momentum are small (i.e., of lower order) compared with those involved in the electron radial momentum, Eq. (16).

The energy balances of ions and electrons provide additional information. The energy integral equations yield

$$\Delta K_i + \Delta R_i = |e\phi_S|,$$
$$\Delta K_e + \Delta R_e = \Delta H_e - |e\phi_S|, \tag{54}$$

where

$$\Delta K_i \simeq m_i u_{riS}^2/2 \simeq T_e/2, \quad \Delta K_e \simeq m_e u_{\theta eS}^2/2,$$
$$\Delta H_e = -T_e \ln(n_S/n_0), \quad \Delta R_i = \int_0^R dr \nu_i m_i u_r, \tag{55}$$
$$\Delta R_e = \int_0^R dr \nu_e m_e u_{\theta e}^2/u_r,$$

are, respectively, the ion and electron kinetic energy gains, the total change on the electron enthalpy, and the ion and electron Joule heating caused by their respective resistive forces. Figure 6 plots the different energy contributions for ions and electrons versus the magnetization strength $\hat{\omega}_{lh}$ for a partially collisional plasma. Observe, first, that, in the MR, electron magnitudes are up to 15 times larger than ion magnitudes. Second, ion resistivity and heating is large in the UR and totally negligible in the MR. Third, the change of electrostatic energy $|e\phi_S|$ is determined by the ion equation. Fourth, $\Delta H_e$ is controlled by $|e\phi_S|$ in the UR (i.e., the Boltzmann equilibrium) and by $\Delta K_e + \Delta R_e$ in the MR. Fifth, $\Delta K_e$ is a contribution to the electron energy losses to the wall: from Eq. (20) one has

$$\hat{E}_W(\hat{u}_{\theta eS}) = \frac{5}{2} + \ln\sqrt{\frac{m_i}{2\pi m_e}} + \Delta K_e, \tag{56}$$

where the first two terms on the right-hand side amount to 7.2 for argon. Moreover, the rise of $\Delta K_e$ to dominant order in the MR makes electron Joule heating, $\Delta R_e$, of dominant order too for $\hat{\nu}_e = O(1)$. Indeed, $\Delta R_e > \Delta K_e$ for $\hat{\nu}_e \gtrsim 0.1$.

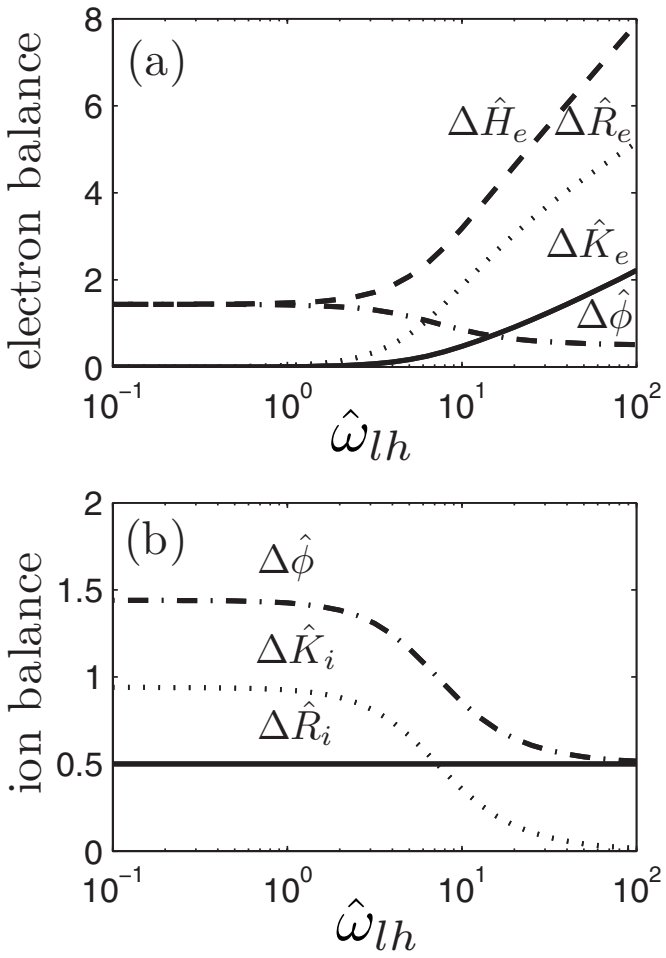


FIG. 6. Energy balance for electrons and ions as function of the magnetization strength for $\hat{\nu}_{in}=\hat{\nu}_{e(n+i)}=3$. Magnitudes are defined in Eq. (55) and are nondimensionalized with $T_e$.

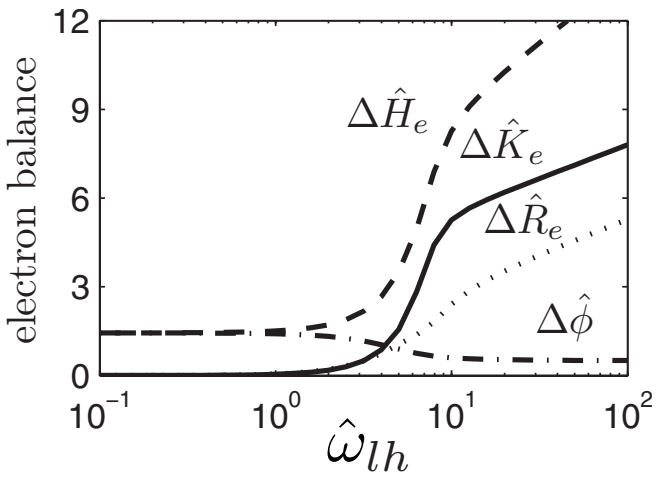


FIG. 7. Energy balance for electrons as function of the magnetization strength for $\hat{\nu}_{in}=3$ and $\hat{\nu}_{e(n+i)}=.01$. Same magnitudes as in Fig. 6.

Figure 7 shows the evolution of the energy balance with $\hat{\omega}_{lh}$ for a low electron collisionality case, $\hat{\nu}_e=0.01$, showing the steepened increase in $\Delta K_e$, $\Delta R_e$, and $\Delta H_e$ within the IR.

#### 1. The Boltzmann relation

Sternberg *et al.*[9] and Allen[8] have argued about the fulfillment of the electron Boltzmann relation near the sheath edge in the MR. Our analysis has shown that, *in all regimes*, the (ambipolar) electric force becomes larger than the magnetic force within the ion-inertial sublayer. This implies that, *in a vicinity of the sheath edge*, Eq. (16) reduces to

$$\frac{d\hat{\phi}}{d\hat{r}}=\frac{1}{\hat{n}}\frac{d\hat{n}}{d\hat{r}}, \tag{57}$$

leading to the Boltzmann relation

$$\hat{n}=\hat{n}_{eS}\exp(\hat{\phi}-\hat{\phi}_S). \tag{58}$$

This last result agrees with the original claim of Allen[8] versus Sternberg *et al.* Later, Allen[10] has suggested that the Bohm criterion would force the fulfillment of the Boltzmann gradient condition (57) *only at the sheath edge S*, but not the Boltzmann relation (58). Our analysis has demonstrated that the Boltzmann relation is indeed satisfied around *S*. It could not be otherwise since the quasineutral plasma behavior is continuous. Therefore, if the electron force balance of Eq. (16) reduces to Eq. (57) at point *S*, this continues to be valid in a vicinity of *S* and thus Eq. (57) can be integrated, yielding the Boltzmann relation.

To end, it is worth to stand out that the fulfillment of the Boltzmann relation around the sheath edge assures the validity of the usual gentle matching of the quasineutral solution and the sheath inner solution, based on the dominance of the electric force. This regular matching (which develops in an intermediate scale[19]) is necessary to validate the outer and inner solutions of our singular perturbation problem. The assertion of Sternberg *et al.*[9] that the Bohm criterion, obtained from the collisionless unmagnetized model, is irrelevant to the problem of a magnetized quasineutral plasma, is certainly not subscribed by us.

### C. Ion and electron collisionality

The parametric analysis shows that ion and electron collisionalities are important *only* in the unmagnetized and magnetized regimes, respectively. In the magnetized regimes, ion resistivity is negligible because it is much smaller than the electron magnetic force, i.e., $\hat{\nu}_i\hat{u}_r\ll\hat{\omega}_{lh}\hat{u}_{\theta e}$ in Eq. (14). To this respect, Figs. 1–7 of Sternberg *et al.* can be confusing, since they show the dependence of the plasma profiles on $\hat{\nu}_i$ in the magnetized regime. The explanation is that, in these figures, $\hat{\nu}_i$ and $\hat{\nu}_e$ are not independent parameters, but they are related by a potential law. Therefore, those plots are indeed showing the dependence on $\hat{\nu}_e$.

In fact, a discussion on the most appropriate model for the ion resistivity is of interest only for the unmagnetized regime. Sternberg *et al.* work with $\nu_i/u_r=\text{const}=\nu_{iS}$ instead of $\nu_i=\text{const}$. Their choice is appropriate for a low-temperature plasma where ion-neutral collisions dominate the ion resistivity, that is $\nu_i\simeq\nu_{in}\gg\nu_w$. For $\hat{\nu}_{iS}\gg 1$, it leads to[7] $\hat{\nu}_w\approx 2.2\hat{\nu}_{iS}^{-1/2}$ and $\hat{n}_S\approx 0.8\hat{\nu}_{iS}^{-1/2}$, instead of the scalings of Eq. (42). The parametric transition to the magnetized regimes is modified accordingly.

In the magnetized regimes, the attention should be on the expression for electron collisionality. For a weakly ionized, hot plasma, with $\nu_e \simeq \nu_{en}$, the assumption $\nu_e = \text{const}$ is reasonable. For a fully ionized plasma, with $\nu_e \simeq \nu_{ei}$, a better assumption would be $\nu_e/n_e = \text{const} = \nu_{e0}$, in order to reflect the strong radial decay of electron collisionality. Computations with this modified model show a moderate decrease in the production frequency and the wall flux; the reason is that $\nu_e \sim \nu_{e0}$ except near the Debye sheath.

### D. The zero-Debye length hypothesis

A central element of the present model (and previous, related works) is the validity of the zero Debye-length assumption. This condition is specially challenged in the MR, where the plasma density drops dramatically near the sheath edge. The zero-Debye length limit or, in other words, the neglect of the space-charge field contribution in the Poisson equation, requires that $\lambda_{dS}^2 \ll \ell_e^{*2}$, where $\lambda_{dS}$ is the Debye length at $S$ and $\ell_e^*$ the gradient length of the quasineutral plasma near $S$. Using Eqs. (29) and (35), the above condition reads

$$\frac{\lambda_{d0}^2}{\ell_e^2} \ll \frac{\hat{\omega}_{lh}^2}{\hat{\nu}_e} \ln \frac{\hat{\omega}_{lh}}{\hat{\nu}_e}, \tag{59}$$

with $\lambda_{d0}$ the Debye length at the axis. This condition can be very restrictive for strong magnetization. Its failure implies that non-neutral effects appear already within the inertial layer, so that the inertial and Debye layers must be treated as a single region. This finite-Debye length problem (not studied here) is similar in nature to the Chodura–Debye sheath problem in an obliquely magnetized plasma[12,14] and to the simpler collisional-sheath problem in an unmagnetized plasma.[20]

## ACKNOWLEDGMENTS

This work was supported by the Gobierno de España (Plan Nacional de I+D+i, Project No. ESP2007-62694) and the 7th Framework Program of the European Community (Grant No. 218862).

[1] L. Tonks, Phys. Rev. **56**, 360 (1939).
[2] W. Schottky, Phys. Z. **25**, 635 (1924).
[3] D. Bohm, *The Characteristics of Electrical Discharges in Magnetic Fields* (McGraw-Hill, New York, 1949), p. 77.
[4] J. Forrest and R. Franklin, Br. J. Appl. Phys. **17**, 1061 (1966).
[5] H. Ewald, F. Crawford, and S. Self, J. Appl. Phys. **38**, 2753 (1967).
[6] L. Tonks and I. Langmuir, Phys. Rev. **34**, 876 (1929).
[7] N. Sternberg, V. Godyak, and D. Hoffman, Phys. Plasmas **13**, 063511 (2006).
[8] J. Allen, Phys. Plasmas **14**, 024701 (2007).
[9] N. Sternberg, V. Godyak, and D. Hoffman, Phys. Plasmas **14**, 024702 (2007).
[10] J. Allen, Contrib. Plasma Phys. **48**, 400 (2008).
[11] J. Gilland, R. Breun, and N. Hershkowitz, Plasma Sources Sci. Technol. **7**, 416 (1998).
[12] E. Ahedo, Phys. Plasmas **4**, 4419 (1997).
[13] E. Ahedo and D. Escobar, Phys. Plasmas **15**, 033504 (2008).
[14] E. Ahedo and D. Carralero, Phys. Plasmas **16**, 043506 (2009).
[15] S. Self and H. Ewald, Phys. Fluids **9**, 2486 (1966).
[16] R. Chodura, Phys. Fluids **25**, 1628 (1982).
[17] K. Riemann, Phys. Plasmas **1**, 552 (1994).
[18] S. M. Tysk, C. M. D. J. E. Scharer, and K. Akhtar, Phys. Plasmas **11**, 878 (2004).
[19] K. Riemann, Phys. Plasmas **4**, 4158 (1997).
[20] J. Blank, Phys. Fluids **11**, 1686 (1968).